PORT SAID ENGINEERING RESEARCH JOURNAL
Faculty of Engineering - Port Said University
Volume 29 No. 1 pp: 69:80

Durability and Steel Corrosion Resistance of Fly Ash- Based Geopolymer Concrete Exposed to Water of Lake Qaroun

Hala Emad Elden Fouad[1, *], *Mohamed Ahmed Bayomy*[2]

[1] *Assistant Professor, Construction Engineering Department, Faculty of Engineering, Misr University for Science and Technology, Egypt., email: hala.fouad@must.edu.eg*
[2]*Assistant Professor, Civil Engineering Department, Faculty of Engineering, Fayoum University, Egypt, email: mab01@fayoum.edu.eg*
**Corresponding author,* *DOI: 10.21608/PSERJ.2024.305550.1353*

Received 18-7-2024
Revised 23-9-2024
Accepted 14-10-2024

ABSTRACT

This paper proposes replacing Ordinary Portland Cement (OPC) with a geopolymer (GP) material made from fly ash (FA) combined with an activator solution as a binding agent. The study investigates the effectiveness of fly ash-based geopolymer concrete (GPC) in aggressive environments, particularly under the conditions of Qaroun Lake. Initially, samples of GPC and OPC were prepared and cured for 28 days, followed by submersion in either aggressive media or potable water for 90 days. To evaluate the durability of the samples, energy-dispersive X-ray spectroscopy (EDX), scanning electron microscopy (SEM), and compression testing were performed. The Linear Polarization Resistance (LPR) technique was used to measure the corrosion rate of steel embedded in concrete samples. The results demonstrate that after 90 days of exposure to Qaroun water, the FA 400, FA 450, and FA 500 samples showed substantial increases in compressive strength (Fcu) by 20.5%, 42.1%, and 42.3%, respectively. The highest compressive strength values were observed in fly ash-based GPC, followed by OPC. Increasing the fly ash (FA) content in GPC enhances its performance. Additionally, GPC exhibits significantly higher compressive strength (CS) compared to OPC. In aggressive environments, the compressive strength of GPC increased nearly threefold compared to that in potable water. Furthermore, the GPC model exhibited a corrosion rate for steel that was approximately 180 times lower than that of the OPC model. The GPC matrix also demonstrated a more stable microstructure under harsh conditions compared to OPC. Microstructural analysis confirmed that GPC maintained a stable mineral composition when subjected to severe attack, whereas OPC did not.

Keywords: Geopolymer concrete; Fly ash; Qaroun water; Steel corrosion; SEM; EDX

1 INTRODUCTION

In the past few decades, construction activities have spread across the globe, inflicting major environmental problems that have a negative impact on human health. Cement is the predominant component of concrete, which contributes to elevated CO_2 quantity in the atmosphere, which causes the greenhouse effect, which has a devastating impact on the environment. The present research has focused on finding an alternative to OPC for minimizing CO_2 emissions. Additionally, to maximize the utilization of raw materials rather than finding a method for disposing of them [1, 2]. GPC is a novel, unconventional solution that considers environmental sustainability and has substantially boosted mechanical characteristics over OPC concrete [3]. Geopolymer (GP) encompasses numerous positive aspects over OPC, including being an eco-friendly, cost-effective, and durable material that can efficiently be utilized to produce high-strength concrete [4, 5]. Two main elements can be utilized to form GP: activator solution as a binder material as well as base material. The latter consists of byproduct materials or waste abundant in alumina and silica, whereas the activator solution is predominantly composed of sodium along with potassium-based substances [6]. When reactive base materials are swiftly dissolved in an activator solution, polymerization occurs [6, 7].

FA is a finely divided ash generated by pulverized coal in power plants and is regarded as an industrial byproduct composed primarily of solid or porous spherical particles. These particulates include crystalline as well as amorphous constituents, such as quartz (SiO_2) and mullite ($3Al_2O_3.2SiO_2$). Alumina typically varies between (20% and 30%), and silica between (40% and 60%). The majority of samples are generated utilizing FA (with a diminished calcium content-class F) per ASTM C 618. [8]. Most studies theoretically investigated the impacts of potassium (K^+) and sodium (Na^+) ions present in potassium hydroxide (KOH) and sodium hydroxide (NaOH), respectively [9]. The reaction between calcium carbonate and NaOH produces a dried alkali activator consisting of calcium hydroxide as well as carbonate of sodium. As an infill, calcium carbonate enhances CS and diminishes porosity [10]. With respect to concrete mechanical properties: CS is enhanced when FA was utilized as A GP base rather than OPC (by 1.5 times) [11,12]. Furthermore, Naidu [13] illustrated that the CS of Fly Ash - Geopolymer Concrete (FA-GPC) attained 90 % (in 14 days) at ambient temperature, from a final value of 57 MPa. FA-GPC has outstanding CS and is appropriate for the products of precast concrete, according to prior research [14]. Hamdy et al. developed (18 FA GP concrete mixtures) to determine their enhanced mechanical characteristics by 28% in comparison to OPC mixtures [12]. According to [15], CS of GPC elevated along with raising the content of FA.

Researchers have focused on the impact of aggressive media on GPC performance in recent years. Reduced calcium FA-based GPC samples exhibited exceptional durability when exposed (for 180 days) to elevated chloride solution and sulfuric acid concentrations. The bars of implanted steel were protected from corrosion by the matrix of concrete, which acted as practically impermeable substances [16]. Soft white deposits eventually transformed into firm crystals on the samples' surface were also observed [17]. In contrast, the efficacy of copper GPC with the activation of sodium hydroxide in chloride solutions and sulfate exhibited a slight rise in CS, but this increase was insignificant. In addition, the samples' corrosion resistance had been enhanced in the aggressive media [18]. Following seven years of immersion, the samples halted steel bars' corrosion and exhibited Na_2CO_3-activated GPC's outstanding resistance to the corrosive solution, according to supporting research [19]. A further investigation that synthesized GP utilizing Qaroun water found that the specimens' CS enhanced by up to 30% relative to OPC and that steel bars' corrosion rate decreased [20, 21]. Therefore, GPC is considered to have higher durability than traditional OPC mixes because it does not contain portlandite and possesses a minimized calcium content [2, 22,23].

In comparison to OPC, GPs possess superior chemical as well as physical characteristics, emit no noxious gases, and exhibit superior resistance if exposed to aggressive media. Additionally, X-ray diffraction (XRD) results demonstrated that GP had fewer fissures and fractures than OPC [24, 25]. Nevertheless, there is little research examining how Qaroun water impacts the rate of rebar corrosion in reinforced GPC. The present research examines FA-GPC impact compared to OPC on rebar corrosion rate. The restorative conditions of Qaroun water are utilized for comparing freshwater properties. In order to identify the microstructural, mineralogical, chemical, and mechanical properties of GPC specimens, SEM, compressive strength testing, EDX, and X-ray diffraction (XRD) are performed on OPC and GP, and OPC samples. In addition, the Linear Polarization Process (LPR) method is employed for estimating steel bars' corrosion rate.

2 EXPERIMENTAL PROCEDURE

2.1 Materials

This investigation employed fly ash (FA) and ordinary Portland Cement (OPC) as cementitious materials. According to the National Research Center, FA is a fine powder (with a 2.1specific gravity) and a particle size of 70 microns. Table 1 shows the oxide composition of ordinary Portland cement (OPC) and fly ash (FA) as determined by X-ray diffraction (XRD) analysis. FA contains significantly less calcium than OPC but is rich in aluminum and silicon compounds. According to Fig. 1, the XRD analysis of fly ash (FA) showed no distinct peaks; however, there is a significant diffuse peak around 15-30° 2θ. Additionally, several peaks identified as quartz minerals do not participate in the chemical reaction. Additionally, there is a prominent bulge between 18 and 36° 2θ in the XRD patterns of fly ash (FA). These findings indicate that the amorphous phase predominates in FA[26]. The OPC (CEM I/52.5N) used in this study complies with ASTM C150 standards. The alkali activator consists of sodium silicate ($Na_2 SiO_3$) and sodium hydroxide (NaOH), commonly known as caustic soda. NaOH is available in pellet or flake form and is highly soluble in water. A 12 molar solution is prepared, consisting of 60.25% Na_2 O, 39.75% water, with a specific gravity of 0.8. The other component of an alkali activator is Na_2SiO_3 developed as a thick liquid or solid. The Na_2SiO_3 utilized in this study is composed of 57 % water, 31.7 % $SiO_3$1, and 1.98 % Na_2O, with a 1.2. specific gravity. As a coarse aggregate, pulverized dolomite with a specific gravity maximum of 2.6- and 12-mm particle size is utilized. Both coarse and fine aggregates are in accordance with the quality and grading requirements of ASTM-C33. The water used for casting or curing the samples was fresh and free from impurities, including organic compounds, acids, oils, and salts in accordance with ASTM D 1193, the water was also free from silt, clay, and other substances that could adversely affect the concrete or reinforcing steel. The pH of the mixing water was 7. The water used in the Qaroun water curing series was sourced from Qaroun Lake in Al-Fayoum. The chemical composition of this water is provided in Table 2.

High-grade tensile carbon steel (12 mm diameter) with a 360 MPa yield strength is utilized.

Table 1. Oxide composition % of the raw material's weight based on X-ray Fluorescence analysis.

Constituents wt.%	OPC	Fly ash
SiO_2	21.70	60.95
Al_2O_3	6.30	29.58
CaO	64.50	1.88
Na_2O	0.28	0.24
Fe_2O_3	3.40	3.54
MgO	1.86	0.14
K_2O	0.54	1.06
Cl	0.00	0.05
SO_3	1.77	0.25
Losses	0.81	0.19

Table 2 The chemical components of Qaroun Lake water.

Property	Result
Density	1.025gm/cm^3
Chlorides	12.985 gm/l
Sodium	10.109 gm/l
Sulfate	9.712 gm/l
Magnesium	1.325 gm/l
Calcium	0.500 gm/l
Bicarbonate	0.305 gm/l
Carbonates	0.030 gm/l
Others	0.472 gm/l
Ions	-

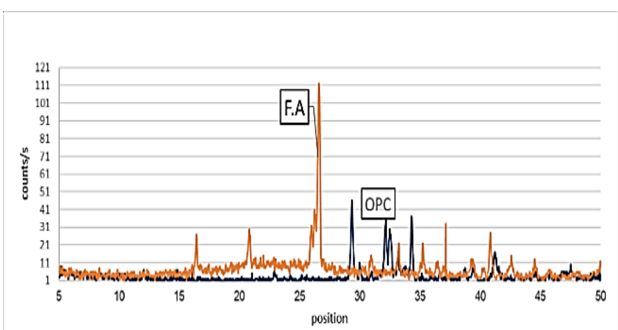

Figure 1: Mineral composition between OPC and FA.

2.2 Concrete mix design, Mixing, and Treatment

This study utilized one OPC concrete mix and three distinct FA concrete samples. Each of FA sample content is FA 400, FA 450, and FA 500 (400, 450, and 500 kg/m^3, respectively), with NaOH: Na_2SiO_3 (1:3 ratio). The ratio of solution proportion to binder (W/G) for all the mixtures of GPC was 0.50 by weight (in order to yield adequate workability) designed according to the ACI-211-11 standards. In contrast, the reference mix OPC includes a w/c 0.50 ratio and 400 kg/m^3 cement. The ratio of coarse aggregate to fine aggregate is (0.65:0.35). Table 3 depicts the ingredients of the mixture (for 1 m^3 of GPC). It is important to note that the steel bars were initially coated with an epoxy zinc primer, except for two 1 cm sections that were left bare to create a closed electrical circuit. All blends were mechanically mixed for 3 minutes, then molded and vibrated for 30 seconds to remove entrapped air. The samples were then covered with plastic wrap to prevent water evaporation and cured at ambient temperature for 24 hours. After demolding, OPC concrete samples were submerged in a water bath for 28 days, while GPC samples were air-cured. Finally, the concrete samples were embedded in an aggressive medium simulating the conditions of Qaroun Lake, while reference samples were left in tap water. The concrete samples were exposed to aggressive median and tap water for a duration of 90 days to evaluate the impact of these media on the durability of the concrete mixes.

Table 3. Mixture components for 1m^3 of GPC mix in (Kg) (with NaOH: Na_2SiO_3=1:3).

Phase	Cement	Fly ash	Sand	Coarse agg.	Total solution
OPC	400	0	595	1190	200
FA400	0	400	595	1190	200
FA450	0	450	558.4	1116.8	225
FA500	0	500	522.3	1044.6	250

2.3 Testing

All four mixtures were subjected to EDX, corrosion rate, SEM, and CS analyses for hardened concrete.

2.3.1 Compressive Strength (CS)

Each of the four mixtures consists of three 10 x 10 x 10 cm³ specimens for compressive strength (CS) testing in aggressive media, resulting in a total of 36 cubic. specimens for comparison with OPC concrete samples. The GPC samples were air-cured, while the OPC samples were water-cured in the laboratory at Fayoum University. The cubes were de-molded after 24 hours and then cured. After 28 days all samples were immersed in the specified water (either Qaroun water or freshwater) for at least three months, as shown in Figure 2.

Figure 2: Concrete cubes specimens exposed to aggressive media.

2.3.2 Corrosion Rate

Forty-eight cylindrical specimens (100 mm in length and 50 mm in diameter), each containing a rebar (100 mm in length and 12 mm in diameter), were used to determine the corrosion rate. The reinforcing bar was positioned vertically in the center of the mold, parallel to its long axis. After molding, the samples were extracted and treated. The corrosion rate was measured by submerging the samples in either freshwater or Qaroun water, stored in plastic containers, for periods of one day, one month, two months, and three months.

The accelerated corrosion method was implemented. The purpose of this method is to promote corrosion by anodically polarizing the steel rod in the concrete specimen. According to [26], the electrochemical circuit received a current density (1 mA/cm^2) from a 12-V direct current (DC) power supply. As depicted in Fig. 3 (a), the stainless steel plate was attached to the power supply negative terminal, and the positive terminal was attached to the reinforced steel bar [26]. The first functions as the anode, whereas the second is the cathode. The electrochemical process details are depicted in Fig. 3 (b) [26].

The cylindrical concrete specimens exposed to aggressive environments are shown in Fig. 4. The gradual increase in corrosion will subject the concrete structure to stresses, which will appear as fractures. Once the accelerated testing was completed, the cylinders were transferred for linear polarization resistance (LPR) corrosion analysis The corrosion rate was determined using a corrosion vessel and the linear polarization resistance (LPR) test with the VOLTAMASTER 4 program, following ASTM C 876. The Tafel extrapolation technique was employed, and polarization experiments were conducted at a scan rate of 5 mV/s.

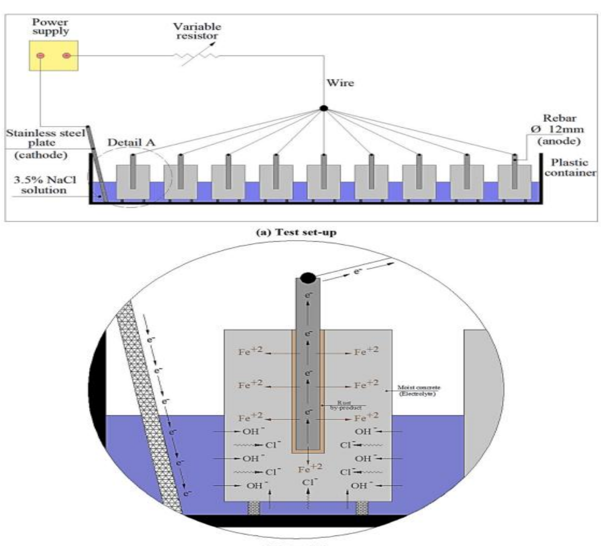

Figure 3: Schematic diagram of the accelerated corrosion technique [32].

Figure 4: Concrete cylindrical specimens exposed to aggressive media.

2.3.3 Instrumentation

The cubic samples were cured for 28 days, then they were exposed to the aggressive media for 1 day, 1 month, 2 months and 3 months. After compressive strength test, the samples were tested at a loading rate of 100 kPa/s. Crushed fragments from the compressive strength tests, after 90 days of immersion, were collected for further analysis using FTIR and SEM. A Perkin Elmer FTIR Spectrum RX1 Spectrometer was used to evaluate the functional groups present in the samples. The samples were ground and mixed with a small amount of potassium bromide, then pressed into 13 mm diameter disks at a pressure of 8 t/cm² for FTIR analysis. The wavenumber range used was 400 to 4000 cm^{-1}. The microstructure of the hardened specimens was examined using an SEM Inspect S (FEI Company, Netherlands) equipped with an energy dispersive X-ray analyzer.

The scanning electron microscope (SEM) is used to characterize and describe the crystallography, composition, and morphology of a specimen's microstructure. In this research, the microscopic characteristics of the samples were determined by analyzing finely pulverized material. To obtain images with high brightness, contrast, and resolution while preventing surface charging, procedures described in [2] were followed. Energy-dispersive X-ray spectroscopy (EDX) is another analytical technique used to characterize and analyze the chemical composition of samples. It operates on the principle that each element in the periodic table has a unique atomic structure, which produces a distinctive set of peaks in its electromagnetic emission spectrum. The EDX analysis was performed using the same semiconductor detectors employed in the SEM study [27].

3 RESULTS AND DISCUSSION

3.1 Compressive strength results when exposed to Qaroun water-aggressive media

OPC concrete samples were cured by submerging them in water for 28 days, while GPC samples were air-cured. Subsequently, both concrete samples were embedded in an aggressive medium (fresh water or Qaroun Lake water). The exposure period to the aggressive medium was 1 day, 1 month, 2 months, and 3 months. Table 4 presents the relationship between the compressive strength of the hardened concrete samples and their immersion time in the different media (after 28 days of curing).

Table 4. The concrete mixtures' CS exposed to a) fresh water and b) Qaroun water.

Concrete sample		OPC	F400	F450	F500
a) Fresh water series	F_{cu} (MPa) 1 day	29.5	39	43.9	50.1
	F_{cu} (MPa) 1 month	30.2	40.1	44.1	53
	F_{cu} (MPa) 2 months	31.6	42	45.3	57.2
	F_{cu} (MPa) 3 months	32	44.3	49	60.5
b) Qaroun water series	F_{cu} (MPa) 1 day	29.5	39	43.9	50.1
	F_{cu} (MPa) 1 month	28.2	43.9	52.8	59
	F_{cu} (MPa) 2 months	26	44.8	56.6	68.4
	F_{cu} (MPa) 3 months	24	47	62.4	71.3

Fig. 5(a) compares GPC and OPC samples' compressive behaviors. In Fig. 5(a), GPC samples with varying FA contents exhibited an increase in compressive strength. This enhancement, particularly evident at higher FA levels, can be attributed to the readily available silica and alumina within the geopolymer matrix. A comparison of the data in Table 4 indicates that the FA 500 sample consistently exhibited the highest compressive strength (CS) compared to the other samples over time. Upon graphical analysis of these results, it is clear that the compressive strength (Fcu) increased by approximately 20% in water. Nonetheless, OPC only resulted in an increase in compressive strength (Fcu) of about 8%, as shown in Table 4 [27]. The compressive strength of each mixture improved over time, particularly with increased FA content. This aligns with the findings of Hala et al. [2], which illustrated that the performance of GPC is largely time-dependent.

The treatment of GPC samples in Qaroun water showed significant strength gains over time. After 90 days, the control mix of OPC exposed to Qaroun water exhibited a decrease in Fcu of approximately 18.6%. In comparison to cement treated in pure water, cement treated in Qaroun water demonstrated lower strength. The presence of chloride ions in Qaroun water facilitated the early formation of calcium hydroxide, consistent with reports in [24-25]. This study used treated Qaroun water as a baseline to assess the impact of FA-GPC on Fcu, as shown in Fig. 5(b). The three levels of FA content examined in the GPC were found to enhance performance in saline conditions, as indicated in [2]. Overall, GPC based on fly ash exhibited more significant improvements in strength compared to OPC concrete. For example, the FA 400, FA 450, and FA 500 samples showed significant increases in compressive strength (Fcu) 90 days after exposure to Qaroun water, reaching 20.5%, 42.1%, and 42.3%, respectively. The highest compressive strength values were observed when fly ash was used as the primary material, followed by ordinary Portland cement (OPC).

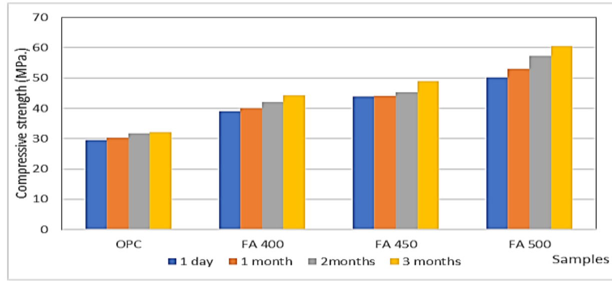

a)

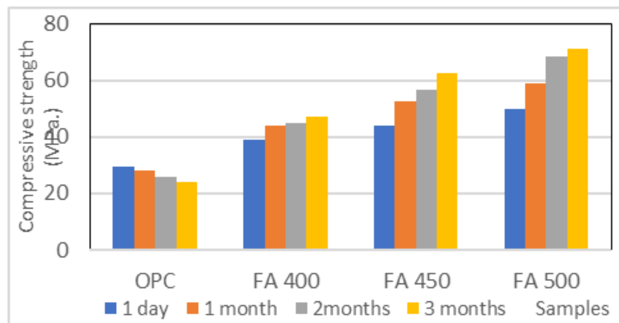

b)

Figure 5: CSs of concrete specimens exposed to (a) freshwater and (b) Qaroun water.

3.2 The corrosion rate results

Figure 6 and Table 5 illustrate how the polarization curves for the mixtures treated with Qaroun water and freshwater were obtained. The OPC sample exhibited a corrosion current nearly 700 times greater than that of GP. It has been confirmed that treating the OPC sample with Qaroun water increases its moisture content. This then acts as an electrolyte medium between the anodic and cathodic portions of the rebar, accelerating corrosion, which is consistent with Dasar et al. [28]. GPs can exhibit greater improvements in compressive strength (CS) compared to OPC samples, as indicated by the corrosion rate. After 90 days of exposure to Qaroun water, the F500 sample's polarization resistance decreased from 1600 to 131.65 Ω·cm², the corrosion current dropped from 80.96 to 60.10 μA/cm², and the corrosion rate reduced significantly from 939.60 to 1.09 mm/year. According to the results presented, the administration of GPC raises the corrosion rate under Qaroun water conditions. In general, OPC samples display much higher rates of corrosion in saltwater media compared to GP samples. It is essential to observe that OPC has two mechanisms for corrosion protection.

Using CH's elevated alkalinity, the first mechanism entails the formation of a passive layer on the steel surface [29, 30].

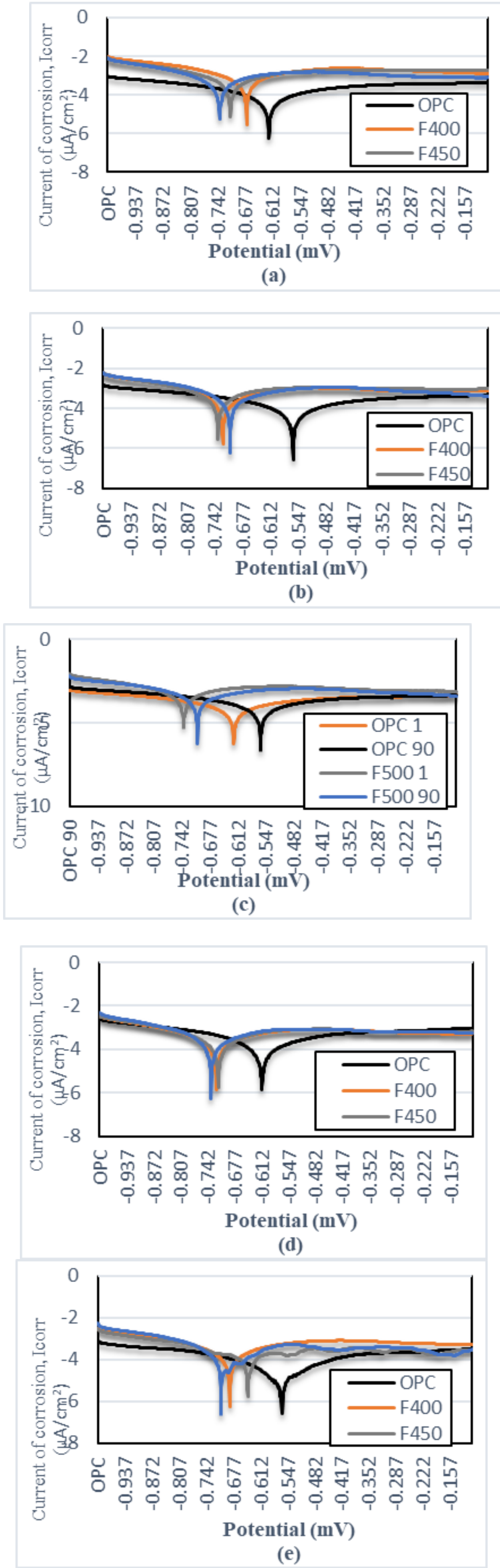

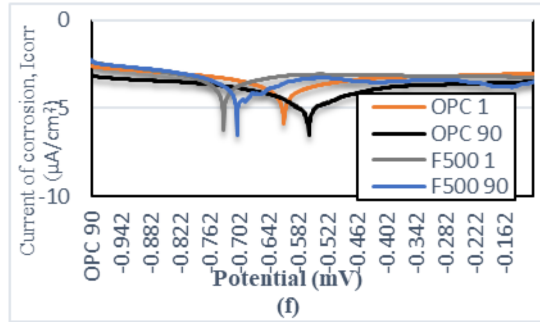

Figure 6: The polarization curves for a) Fresh water at Day 1, b) Fresh water at Day 90, c) Freshwater compares at Day 1 and Day 90, d) Qaroun water at Day 1, e) Qaroun water at Day 90 and f) Qaroun water compares at Day 1 and Day 90.

Table 5. Corrosion analysis parameters' data for a) fresh water, and b) Qaroun water treated series.

Case study		a) Freshwater treated series			
		OPC	**F400**	**F450**	**F500**
a) At 1 day	E_{corr} (mV)	-621.60	-674.30	-712.30	-737.70
	Rp ($\Omega.cm^2$)	607.71	58.73	69.81	79.01
	I_{corr} ($\mu A/cm^2$)	43.70	0.428	0.3997	0.3291
	Corrosion rate (mm/ year)	507.50	4.969	4.639	3.82
b) at 28 days	E_{corr} (mV)	-640.10	-728.60	-704.40	-690.70
	Rp ($\Omega.cm^2$)	422.05	88.40	83.57	88.73
	I_{corr} ($\mu A/cm^2$)	44.37	0.322	0.31	0.30
	Corrosion rate (mm/ year)	515	3.74	3.70	3.488
c) at 90 days	E_{corr} (mV)	-559.10	723.40	-734.20	-706.10
	Rp ($\Omega.cm^2$)	550.68	130.32	98.48	115.39
	I_{corr} ($\mu A/cm^2$)	48.29	0.2817	0.2699	0.2641
	Corrosion rate (mm/ year)	560.40	3.269	3.133	3.07
Case study		**b) Qaroun water treated series**			
		OPC	**F400**	**F450**	**F500**
a) at 1 day	E_{corr} (mV)	-611.5	-721.2	-716.6	-733.80
	Rp ($\Omega.cm^2$)	329.2	168.5	161.2	155.76
	I_{corr} ($\mu A/cm^2$)	61.74	162.5	153.4	147.76
	Corrosion rate (mm/ year)	716.5	1.886	1.78	1.715
b) at 28 days	E_{corr} (mV)	-631.8	-697.2	-720.6	-673.40
	Rp ($\Omega.cm^2$)	363.7	183.4	187.9	142.89
	I_{corr} ($\mu A/cm^2$)	72.55	137	232.6	125.39
	Corrosion rate (mm/ year)	842.1	1.59	1.49	1.455
c) at 90 days	E_{corr} (mV)	-561	-686.2	-642	-729.50
	Rp ($\Omega.cm^2$)	1600	199.5	196.8	131.65
	I_{corr} ($\mu A/cm^2$)	80.96	133.6	120.7	60.1
	Corrosion rate (mm/ year)	939.6	1.55	1.40	1.09

The second mechanism involves the use of C-S-H gel's blocking properties to keep the steel matrix physically protected [31,32]. Due to the fact that GP samples have a greater density (higher CS) and pH value than OPC samples, they are more resistant to corrosion. Moreover, it is more resistant to intake by NC-NS media and degradation by MC-MS media. Additionally, the presence of FA prevents chloride ions from accessing reinforcement [33, 34]. Consequently, the F500 sample performs the best due to its deficient CaO concentration. This precludes the formation of calcium carbonates, and thus no white deposits (salt) formed. Alternatively, OPC samples with an elevated concentration of CaO reacting with carbon dioxide produced calcium carbonate compounds [33, 34]. Given that the immersion media are not permitted to penetrate the reinforcement, the topmost surfaces of the samples are exposed to air. Fig.7 depicts the specimens that were exposed to Qaroun water media.

a)**OPC** b)**F500**

Figure 7: Photos of samples after exposure to Qaroun water media for 90 days for a) OPC, and b) F500.

3.3 SEM analysis

Following the compressive strength (CS) testing, scanning electron microscopy (SEM) micrographs were obtained from all exposed samples immersed in Qaroun water and freshwater. Fig. 8 (a) depicts the POC non-crystalline (amorphous) matrix following freshwater treatment. CH manifests as hexagonal crystals, calcium silicate hydrate as gel, and ettringite as needles, with a notable number of cavities and fractures. In comparison to F 400 and F 500, OPC most closely resembles portlandite, which decomposes into magnesium silicate hydrate, sodium, and gypsum. Moreover, as ettringite density increases, porosity declines markedly [35]. Even though the crystalline particles are well-formed as well as translucent, unreacted FA particles continue to exist in the structure, as shown in Figs. 8(b) and 8(c) from the F 400 and F 500 matrix treated with fresh water. The FA particles range in size from 1 to 10 m and have a uniform, spherical shape.

A component with an elevated atomic number corresponds to the vibrant color, while a constituent element with a minimal atomic number corresponds to the dark color [36]. In a heterogeneous, porous matrix, FA-based GP is composed of residual alkaline precipitates, GP gel, and partially or non-reacted FA grains. GPC is composed of a dense, continuous gel-like structure with readily visible micropores and microcracks at the surface level. Increasing FA content decreases fractures and fissures and increases GP gel, increasing strength. On the GPC binder's surface, the unreacted alkali solution containing FA spheres can occasionally cause the formation of tiny needle- or stripe-shaped particulates. The spines of the reaction products form the bonds between grains, and the crust's attachment to the sphere does not appear to be particularly strong [37]. Therefore, pores are visible in significantly decreased concentrations than OPC [38].

In Fig. 9 (a), a Qaroun water-treated OPC sample contains numerous CH crystals, needles, and massive cavities, resulting in a porous structure. Additionally, slabs of calcium silicate hydrate (C-S-H) are distinguishable. Fig. 9(b) depicts the influence of FA on the GP matrix following immersion for 90 days. Additionally, sodium sulfate deposits are evident. This occurred due to sodium ions permeating the matrix. The amorphous structure has also partially transformed into a crystalline form. This can be explained by immersion duration, which could be responsible for the increased CS of the exposed samples [39]. Fig. 9(c) demonstrates elevated FA content impact on the GP matrix following immersion for 90 days. Magnesium ion leak into the matrix can be detected, which is responsible for the sporadic occurrence of Si-Al gel and some Mg in the matrix. This modification does not appear to affect the gel's potency [40] significantly.

3.4. EDX analysis

Figures 10 and 11 depict the mapping images provided by the fresh water and Qaroun water-treated mixtures (OPC, F 400 and F 500), while Figure 12 demonstrate the corresponding EDX spectra. In addition, Tables 6 & 7 list the matching individual chemical components as well as the expected chemical compounds of these mixtures, respectively. The atoms of alumina, oxygen, silica, calcium, and carbon were found to be the fundamental elements in every group. The calcium content of the OPC sample treated in freshwater was 51.04 percent, while it was 6.88 percent in F 400 and 4.7 percent in F 500. For instance, the silica content of the OPC specimen treated with fresh water was 3.72 percent, while it rose to 25.91 percent in F 400 and 27.36 percent in F 500. The alumina content of the OPC specimen treated in freshwater was 0.56%, increased to 6.47% in F 400, but decreased to 6.66% in F 500. Based on the EDX analysis, the most probable chemical compounds for the GP groups were silicon oxide and aluminum oxide, whereas, for the control group, it was calcium carbonates or (calcium oxide and carbon oxide). In calcium oxide, the F 400 group (9.62%) and F 500 group (6.58%) exhibited decreased compound than the OPC group (71.41%).

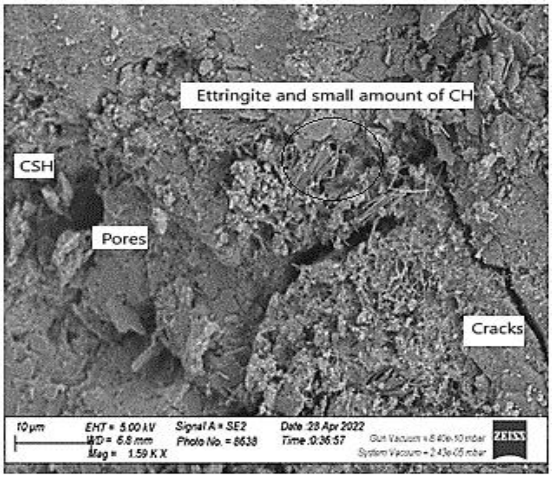

a) **OPC**

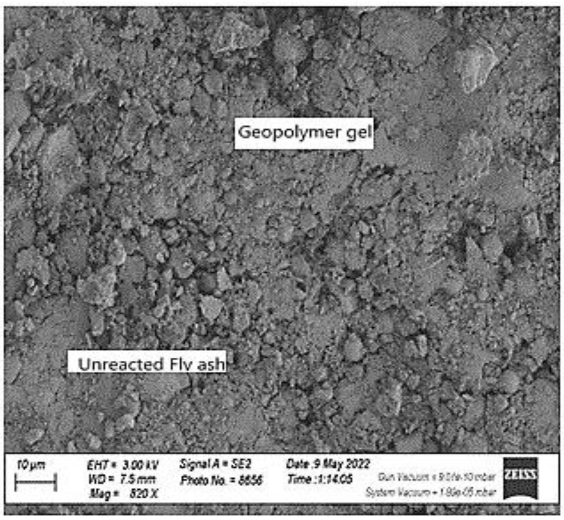

b) **F400**

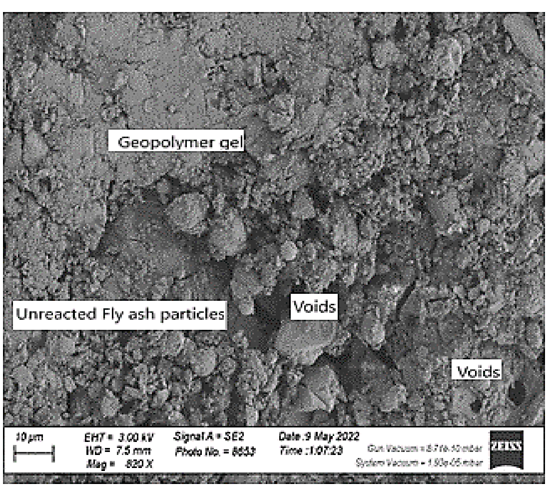

c) **F500**

Figure 8: SEM of the freshwater treated specimens, a) OPC, b) F400 and c) F500.

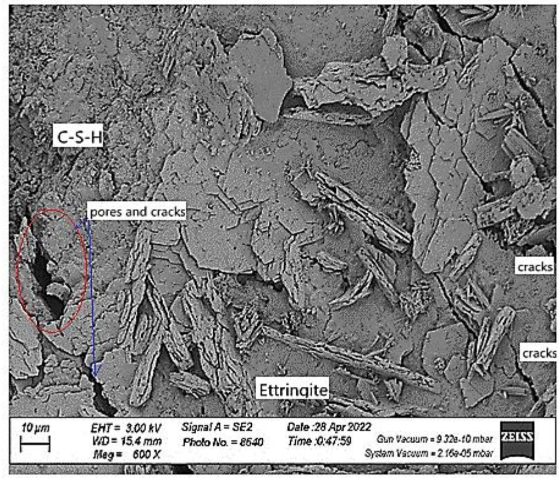

a) OPC

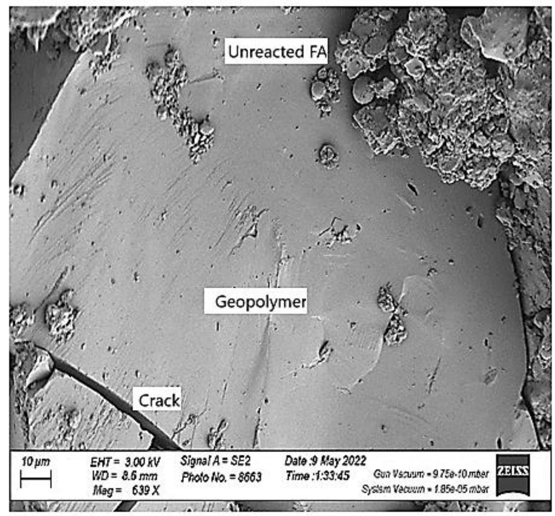

b) F400

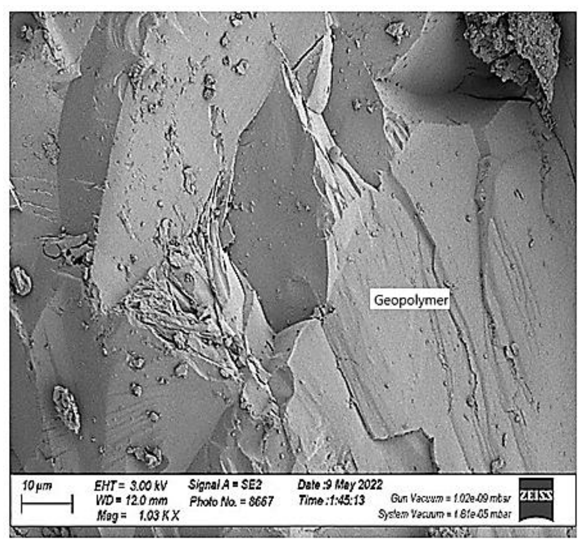

c) F500

Figure 9: SEM of the Qaroun water treated specimens, a) OPC, b) F400 and c) F500.

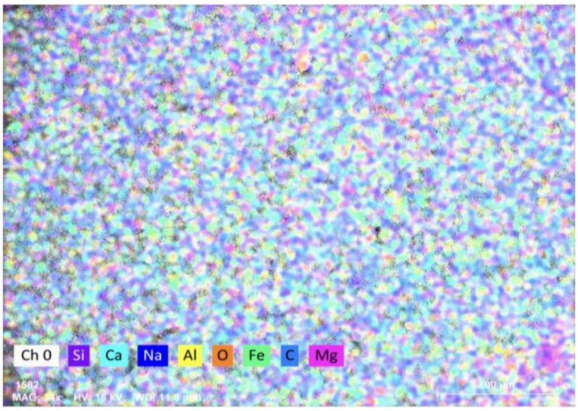

a)OPC

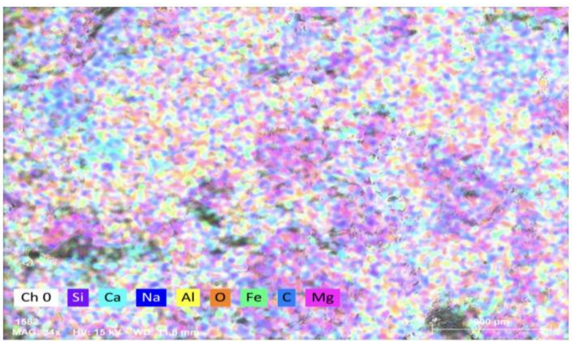

b) F400

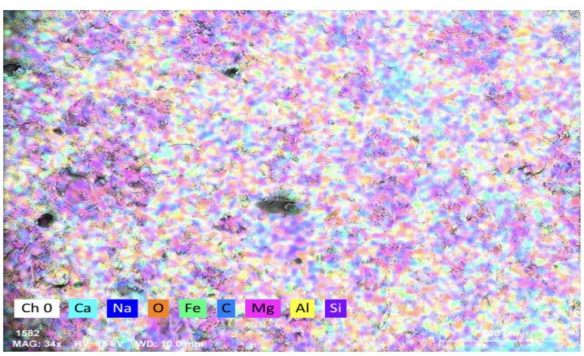

c)F500

Figure 10: Mapping images of the freshwater treated OPC, F 400, and F 500 specimen's chip.

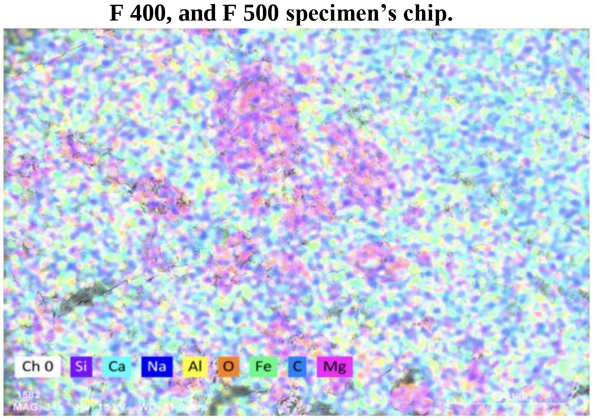

a)OPC

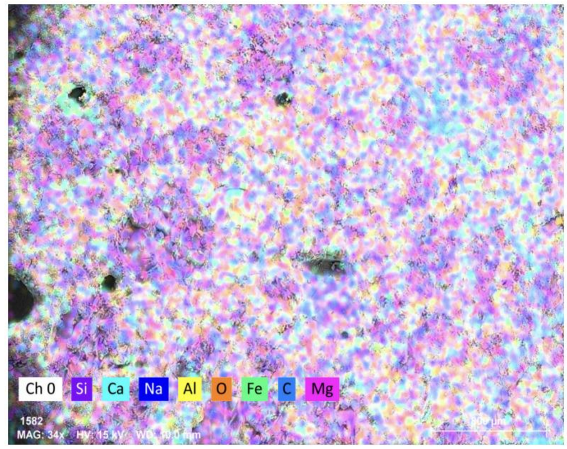

b)F400

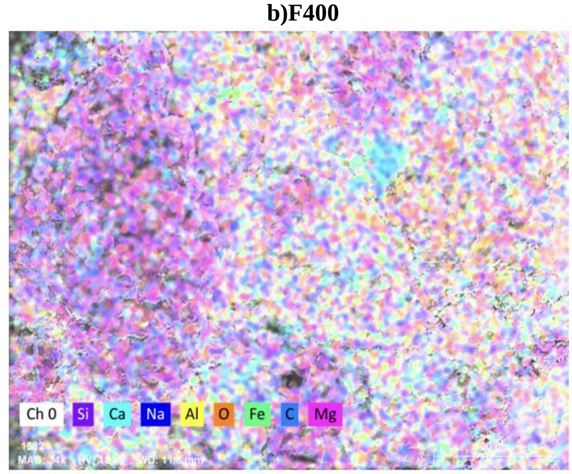

C)F500

Figure 11: Mapping images of the Qaroun water treated OPC, F 400, and F 500 specimen's chip.

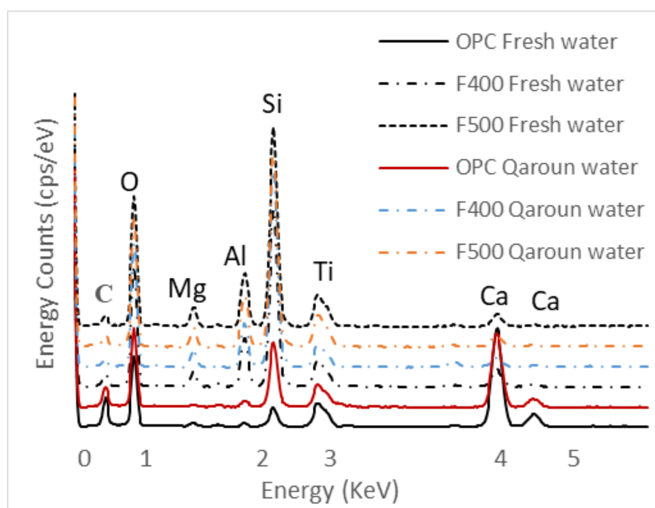

Figure 12: EDX spectra of the fresh and Qaroun water treated OPC, F 400, and F 500 specimens.

Table 6: The chemical components of the fresh- and Qaroun water-treated series by EDX.

Elem.	a) Freshwater treated series					
	OPC		F400		F500	
	Weight %	Atoms %	Weight %	Atoms %	Weight %	Atoms %
Si	3.72	2.93	25.91	17.20	27.36	18.19
Ca	51.04	28.18	6.88	3.20	4.70	2.19
Na	1.12	1.08	2.72	2.20	3.19	2.59
Al	0.56	0.46	6.47	4.47	6.66	4.61
Fe	0.48	0.19	1.26	0.42	1.57	0.52
O	25.92	35.84	39.71	46.27	40.87	47.69
C	16.84	31.02	16.75	26.00	15.49	24.08
Mg	0.32	0.29	0.32	0.24	0.15	0.12
	b) Qaroun water treated series					
Elem.	**OPC**		**F400**		**F500**	
	Weight %	Atoms %	Weight %	Atoms %	Weight %	Atoms %
Si	14.76	11.46	30.47	21.00	40.76	29.55
Ca	41.92	22.81	4.04	1.95	6.63	3.37
Na	0.88	0.84	3.12	2.62	4.05	3.59
Al	1.23	0.99	5.99	4.30	9.17	6.92
Fe	1.32	0.51	1.10	0.38	2.50	0.91
O	19.07	25.99	42.79	51.75	13.37	17.01
C	20.39	37.01	10.57	17.03	22.53	38.18
Mg	0.43	0.39	0.06	0.05	0.13	0.11

Table 7: The predicted chemical compounds of the fresh- and Qaroun water treated series by EDX.

Elem.	a) Freshwater treated series			b) Qaroun water treated series		
	OPC	F400	F500	OPC	F400	F500
SiO2	7.95	55.42	58.54	31.58	65.19	40.76
CaO	71.41	9.62	6.58	41.92	5.66	9.27
Na2O	1.51	3.67	4.30	1.19	4.20	5.46
Al2O3	1.07	12.22	12.59	2.32	11.33	17.32
Fe2O3	0.68	1.80	2.24	1.88	1.10	3.58
MgO	0.53	0.52	0.26	0.71	0.10	0.21
CO	9.83	16.75	15.49	20.39	10.57	22.53

Nonetheless, the F 400 group (16.75%) and F 500 group (15.49%) exhibited a greater quantity of carbon oxide compound than the OPC group (9.80%). In addition, the F 400 group (55.42 % &12.22 %) and the F 500 group (58.54 %, 12.59 %) contained a greater quantity of silicon oxide as well as aluminum oxide compounds than the OPC group (7.95 % & 1.07%. However, Qaroun water treatment results in a greater quantity of calcium oxides, alumina, and silicon, along with a reduced amount of calcium oxide in GP samples compared to OPC samples treated in freshwater. This occurrence (elevated alumina, silica, and calcium content) is predominantly responsible for the aforementioned enhancement in the properties of the concrete as a result of FA addition. These findings align with those of Chahal et al. [40]. Furthermore, adding algae to concrete may be a viable option to boost the precipitation of CS and $CaCO_3$, SiO_2, and Al_2O_3. The F 400 and F 500 series are believed to have enhanced the concrete's properties, unlike the Qaroun water-treated OPC series [26].

CONCLUSIONS

As a major component of concrete, OPC contributes significantly to CO_2 emissions, which are harmful to the environment. Previous research has proposed FA-GPC as a sustainable alternative to OPC concrete. However, few studies have investigated the effects of Qaroun water treatment on GPC. In this study, the compressive strength (CS) of GPC exposed to Qaroun water with time, as well as the corrosion rate of steel rods embedded in FA-GPC, were analyzed and compared to OPC concrete. The results show that:

- The FA 500 model provides the highest compressive strength over time compared to other models. By plotting these results, Fcu increases by about 20% in water. However, OPC only improves Fcu by about 8% after 90 days.
- Increasing the FA content in GPC improves mechanical properties and durability.
- Prolonged exposure to aggressive environments enhanced the CS of GPC by up to 42.3% exposed to Qaroun water for 90 days. The GPC samples showed an improvement in compressive strength in aggressive median. So, GPC is more durable than OPC mixtures due to its lack of portlandite and lower calcium content.
- Furthermore, the corrosion rate of steel bars in GPC samples is greatly reduced by approximately 180 times lower than that of the OPC model.
- The chemical responses of OPC and GPC diverge under harsh conditions. The results showed that GPC products have many properties such as voids, porosity, microcracks, FA spheres, dense and large binders, Qaroun water is more important than the freshwater impact, and amorphous materials according to the synthetic FA microstructure.
- GPC offers numerous advantages, including environmental friendliness, cost-effectiveness, durability, and suitability for producing high-strength concrete. So overall, this study shows that the efficacy of GPC is better than OPC.

Recommendations for future researchers: it’s preferable to use different cover thicknesses and different numbers of steel bars in the sample to simulate different structure elements.

Declaration of competing Interest

The authors declare that they have no known competing financial interests or personal relationships that could have appeared to influence the work reported in this paper.

Declaration of Funding

List funding agencies in a standard way to facilitate compliance with the funder's requirements.

Funding: This work was supported by the [Hala Emad Eldeen Fouad Mohamed] grant number [01004310234].

REFERENCES

[1] Zhijun He, Xiaodong Zhu, Junjie Wang, Mulan Mu, and Yuli Wang, "Comparison of CO_2 emissions from OPC and recycled cement production", Construction and Building Materials, 211: 965-973, 2019.

[2] Hala E. E. Fouad, W. H. Soufi, A. S. Elmannaey, M. Abdelaziz and H. Elgazaly," Durability and steel corrosion resistance of slag with metakaolin based geopolymer concrete", Journal of engineering and applied science, Faculty of engineering, Cairo University, Vol. 67, no. 6, PP. 1381-1398, DEC. 2020.

[3] Poem Nuaklong, Ampol Wongsa, Kornkanok Boonserm, Chanchai Ngohpok, Pitcha Jongvivatsakul, Vanchai Sata, Piti Sukontasukkul and Prinya Chindaprasirt, "Enhancement of mechanical properties of fly ash geopolymer containing fine recycled concrete aggregate with micro carbon fiber", Journal of Building Engineering, 41, 102403, 2021.

[4] Mohd M. Abdullah, Liew Yun Ming, Heah Yong and Muhammad Faheem Tahir," Clay -based materials in geopolymer technology", book chapter 14, http://dx.doi.org/10.5772/intechopen.74438. 2018.

[5] F.N. Okoye, J. Durgaprasad and N.B. Singh, " Mechanical properties of alkali activated fly ash/Kaolin based geopolymer concrete," Construction and Building Materials, vol. 98, Pages:685-691, 2015.

[6] M. M. H. Abdeen, M. Abdel Haleem, Medhat Sobhy El-Mahllawy and Hisham Mustafa Khater, "Applied geological studies on some kaolin deposits and industrial wastes for production of nano geopolymer composites", Egypt, Degree of Doctor of Philosophy in Science (Geology), El-Azhar University, 2016.

[7] J. Fernando Pacheco-Torgal and Said Jalali, "Alkali-activated binders: A review Part 1. historical background, terminology, reaction mechanisms and hydration products," Construction and Building Materials, vol. 22, pp. 1305-1314, 2008.

[8] ASTM C618-2019, Standard specification for coal fly ash and raw or calcined natural pozzolan for use in concrete, ASTM International, West Conshohocken, PA (2019).

[9] Tanakorn Phoo, Akihiro Maegawa, Naoki Mishima and Shigemitsu Hatanaka," Effects of sodium hydroxide and sodium silicate solutions on compressive and shear bond strengths of FA–GBFS geopolymer", Construction and Building materials, 91:1-8, 2015.

[10] Jhutan Chandra Kuri, Subhra Majhi, Prabir Kumar Sarker and Abhijit Mukherjee," Microstructural and non-destructive investigation of the effect of high temperature exposure on ground ferronickel slag blended fly ash geopolymer mortars", Journal of Building Engineering, 43, 103099, 2021.

[11] Shaswat Kumar Das, Syed Mohammed Mustakim, Adeyemi Adesina, Jyotirmoy Mishra, Thamer Salman Alomayri, Hasan Suliman Assaedi and Cyriaque Rodrigue Kaze," Fresh, strength and microstructure properties of geopolymer concrete incorporating lime and silica fume as replacement of fly ash.", Journal of Building Engineering, 32, 101780, 2020.

[12] Hamdy K. Shehab, Ahmed S. Eisa and Ahmed M. Wahba, "Mechanical properties of fly ash based geopolymer concrete with full and partial cement replacement," Construction and Building Materials, vol. 126, Pages:560-565, 2016.

[13] P. Ganapati Naidu. P, S.Adiseshu, P.V. Satayanarayana, "A Study on strength properties of geopolymer concrete with addition of G.G.B.S," International Journal of Engineering Research and Development, vol. 2, no. 4, pp. 19-28, 2012.

[14] M. G. Maneeshkumar C S, Prasanth S, "An experimental investigation on GGBS and flyash based geopolymer concrete with replacement of sand by quarry dust," Journal of Engineering Research and Applications, vol. 5, no. 5, pp. 91-95, 2015.

[15] B. Rajini, A.V. Narasimha Rao, "Mechanical properties of geopolymer concrete with fly ash and GGBS as source materials," International Journal of Innovative Research in Science, Engineering and Technology, vol. 3, no. 9, pp. 15944-15953, 2014.

[16] Kannapiran, K., Sujatha, T., and Nagan, S., "Resistance of Reinforced Geopolymer Concrete Beams to Acid and Chloride Migration", Asian Journal of Civil Engineering, Vol. 14, No. 2, pp. 225-238, 2013.

[17] Thokchom, S., Ghosh, P., and Ghosh, S., "Performance of Fly Ash Based Geopolymer Mortars in Sulphate Solution", Journal of Engineering Science and Technology Review, vol.3, no.1, pp. 36-40, 2010.

[18] Deja, J., and Malolepszy, J., "Long-Term Resistance of Alkali-Activated Slag Mortars to Chloride Solution", 3 rd CANMET/ACI International Conference on durability of concrete, Nice, France, (Supplementary Paper), pp. 657–671, 1994.

[19] Kurdowski, W., Duszak, S., and Trybalska, B., "Corrosion of Slag Cement in Strong Chloride Solutions", 1 st International Conference on Alkaline Cements and Concretes, Kiev, Ukraine, Vol. 2, pp. 961–970, 1994.

[20] Bakharev, T., Sanjayan, J. G., and Cheng, Y. B., "Sulphate Attack on Alkali Activated Slag Concrete", Cement and Concrete Research, Vol. 32, No. 2, pp. 211–216, 2002.

[21] Abd El-moatey, A., Faried, A., Soufi, W., and Abd El-Aziz, M.,"Improve the Formation of Geopolymer Concrete Mixed with Seawater and without Treatement",

American Journal of Construction and Building Materials, Vol. 2, No. 4, pp. 78- 85, 2017.

[22] Nan Su, Buquan Miao and Fu-Shung Liu,“Effect of wash water and underground water on properties of concrete”, Cement and Concrete Research vol 32(5), pp.777-782, May 2002.

[23] Qingyong Guo, Lei Chen, Huijian Zhao, Jorge Admilson and Wensong Zhang,“The effect of mixing and treatement sea water on concrete strength at different ages”, MATEC Web of Conferences 142, 02004, 2018.

[24] Salmabanu Luhara, Sandeep Chaudhary and Ismail Luhar,” Thermal resistance of fly ash based rubberized geopolymer concrete.”, Journal of Building Engineering, 19, 420-428, 2018.

[25] Peem Nuaklong, Pitcha Jongvivatsakul, Thanyawat Pothisiri, Vanchai Sata and Prinya Chindaprasirt,” Influence of rice husk ash on mechanical properties and fire resistance of recycled aggregate high-calcium fly ash geopolymer concrete.”, Journal of Cleaner Production, 252, 119797, 2020.

[26] C.V. Nguyen, P. Lambert, “Effect of current density on accelerated corrosion of reinforcing steel bars in concrete.”, Structure and Infrastructure Engineering, 2018, 1-12.

[27] Khaled M. Osman, Fatma M. Taher, Adel Abd EL-Tawab and A. Serag Faried,“Role of different microorganisms on the mechanical characteristics, self-healing efficiency, and corrosion protection of concrete under different treatement conditions.”, Journal of Building Engineering, (2021), 41- 102414.

[28] A. Dasar, D. Patah, H. Hamada, Y. Sagawa, D. Yamamoto, Applicability of seawater as a mixing and treatement agent in 4-year-old concrete, Construct. Build. Mater. 259 (2020), 119692.

[29] Girish, M.G., Shetty, K.K. & Nayak, G. Effect of Slag Sand on Mechanical Strengths and Fatigue Performance of Paving Grade Geopolymer Concrete. Int. J. Pavement Res. Technol. (2023). https://doi.org/10.1007/s42947-023-00363-2

[30] Toutanji, H., Delatte, N., Aggoun, S., Duval, R., and Danson, A., “Effect of Supplementary Cementitious Materials on the Compressive Strength and Durability of Short-Term Treated Concrete”, Cement and Concrete Research, Vol. 34, No. 2, 2004

[31] Hanjitsuwan, S., Hunpratub, S., Thongbai, P., Maensiri, S., Sata, V., and Chindaprasirt, P., “Effects of NaOH Concentrations on Physical and Electrical Properties of High Calcium Fly Ash Geopolymer Paste”, Cement and Concrete Composites, Vol. 45, pp. 9-14, 2014.

[32] Kong, D., and Sanjayan, J., “Effect of Elevated Temperatures on Geopolymer Paste, Mortar and Concrete”, Cement and Concrete Research, Vol. 40, pp.334- 339, 2010.

[33] Siti, M. S., Al Bakri, A. M., Kamarudin, H., Ruzaidi, C. M., Binhussain, M. and Zaliha, S. Z., “Review on Current Geopolymer as a Coating Material”, Australian Journal of Basic and Applied Sciences, Vol. 7, No. 5, pp. 246-257, 2013.

[34] McCaffrey, R., “Climate Change and the Cement Industry”, Global Cement and Lime Magazine: Environmental Special Issue, pp. 15-19, 2002

[35] Neville, A. M., and Brooks, J. J., “Concrete Technology”, 2 nd Edition, Pearson Education, 2010.

[36] Ari Widayanti, Ria Asih Aryani Soemitro, Hitapriya Suprayitno, and Januarti Jaya Ekaputri,"Characterization and compressive strength of fly ash based-geopolymer paste", MATEC Web of Conferences 195, 01023, ICRMCE 2018.

[37] S. Alehyen, M. EL Achouri and M. Taibi," Characterization, microstructure and properties of fly ash-based geopolymer", Journal of Materials and Environmental Sciences ISSN: 2028-2508, JMES, vol 8, Issue 5, pp 1783-1796, 2017.

[38] Shi, C., Krivenko, P., and Roy, D., “Alkali-Activated Cements and Concretes”, 1st Edition, CRC Press, 2003.

[39] Provis, J., and Deventer, J., “Geopolymers Structure, Processing, Properties and Industrial Applications”, CRC Press, 2009

[40] N. Chahal, R. Siddique, Permeation properties of concrete made with fly ash and silica fume: influence of ureolytic bacteria, Construction and building materials, v 49, 161-174, 2013.